Available online at www.sciencedirect.com
ScienceDirect
Journal of the European Ceramic Society 29 (2009) 2549–2557
www.elsevier.com/locate/jeurceramsoc

Analysis of reactions during sintering of CuO-doped 3Y-TZP nano-powder composites

Louis Winnubst [a,*], Shen Ran [b], Emiel A. Speets [c], Dave H.A. Blank [b]

[a] *Inorganic Membranes, MESA+ Institute for Nanotechnology, University of Twente, P.O. Box 217, 7500 AE Enschede, The Netherlands*
[b] *Inorganic Materials Science, MESA+ Institute for Nanotechnology, University of Twente, P.O. Box 217, 7500 AE Enschede, The Netherlands*
[c] *Central Materials Analysis Laboratory, MESA+ Institute for Nanotechnology, University of Twente, P.O. Box 217, 7500 AE Enschede, The Netherlands*

Received 22 November 2008; accepted 20 February 2009
Available online 21 March 2009

Abstract

3Y-TZP (yttria-doped tetragonal zirconia) and CuO nano powders were prepared by co-precipitation and copper oxalate complexation–precipitation techniques, respectively. During sintering of powder compacts (8 mol% CuO-doped 3Y-TZP) of this two-phase system several solid-state reactions clearly influence densification behaviour. These reactions were analysed by several techniques like XPS, DSC/TGA and high-temperature XRD. A strong dissolution of CuO in the 3Y-TZP matrix occurs below 600 °C, resulting in significant enrichment of CuO in a 3Y-TZP grain-boundary layer with a thickness of several nanometres. This "transient" liquid phase strongly enhances densification. Around 860 °C a solid-state reaction between CuO and yttria as segregated to the 3Y-TZP grain boundaries occurs, forming $Y_2Cu_2O_5$. This solid-state reaction induces the formation of the thermodynamic stable monoclinic zirconia phase. The formation of this solid phase also retards densification. Using this knowledge of microstructural development during sintering it was possible to obtain a dense nano–nano composite with a grain size of only 120 nm after sintering at 960 °C.

Keywords: Sintering; Microstructure; Zirconia; Copper oxide; Nanopowder

1. Introduction

CuO-doped yttria-stabilized tetragonal zirconia polycrystals (Y-TZP) ceramic composites have drawn great interest due to their special properties such as superplastic deformation and low friction under dry sliding conditions.[1–4] These properties extend the materials' potential applications into near net shape forming of ceramics[1] and as a solid lubricant.[2–4]

During sintering of CuO-doped Y-TZP systems several reactions occur.[4–11] These reactions have profound influences not only on sintering behaviour but also on the microstructure of the final ceramic. It is observed in course-grained systems that these reactions retard densification[4–6] and result in a tetragonal to monoclinic zirconia phase transformation during sintering.[5–8] The material can even crack during sintering if these reactions are not well controlled.[5,8] A sound knowledge of the reactions between CuO and 3Y-TZP during sintering is important for understanding and controlling the sintering process and microstructure evolution of the material.

For analysing these reactions Seidensticker and Mayo[9] performed DTA and TGA analysis on 3 mol% CuO-doped 3Y-TZP (Tosoh Inc.) powder prepared by an adsorption technique. In this system copper species are supposed to be homogeneously covering the submicrometer 3Y-TZP particles as multi-layer adsorbents. Several reactions such as dissociation of CuO at 1030 °C and melting of Cu_2O at 1140 °C are clearly identified.[9] These authors also claimed that an $Y_2Cu_2O_5$ phase is formed at 1200 °C due to the reaction between the molten Cu_2O and yttria as segregated to the 3Y-TZP grain boundaries. Mayo et al.[10] reported HR-TEM analyses on CuO-doped Tosoh 3Y-TZP systems and claimed that a small amount (<0.3 mol%) of CuO dissolved into the 3Y-TZP grains by forming a Cu-rich grain-boundary layer with a thickness of several nm. It is obvious that the solubility of CuO in a 3Y-TZP matrix is strongly influenced by its grain-boundary volume so ceramic grain size. Hayakawa and colleagues[11] investigated reactions in 3Y-TZP doped with

* Corresponding author. Tel.: +31 53 489 2994; fax: +31 53 489 4611.
E-mail address: a.j.a.winnubst@utwente.nl (L. Winnubst).

0955-2219/$ – see front matter © 2009 Elsevier Ltd. All rights reserved.
doi:10.1016/j.jeurceramsoc.2009.02.009

various amounts of CuO prepared by traditional mixing techniques. Differently from Seidensticker's results,[9] these authors concluded that in their systems the formation of $Y_2Cu_2O_5$ occurs at around 850 °C during heating and that CuO dissolves in the 3Y-TZP matrix at around 1200 °C. The discrepancy between Seidensticker's and Hayakawa's work might be caused by the different characteristics of the powders they used, e.g. particle size and distribution of CuO in the 3Y-TZP matrix. However all these authors used course-grained, (sub) micron-sized powders.

In recent work we have described the densification behaviour of CuO/3Y-TZP powder compacts starting from nanocrystalline CuO and 3Y-TZP powders.[12,13] It is shown that addition of up to 8 mol% of CuO to 3Y-TZP initiates densification at a much lower temperature, resulting in full density at lower temperature if compared with pure 3Y-TZP. In this paper investigations are described of the several reactions as occur in compacts of these CuO-doped 3Y-TZP nano-powder composites. For analysis of these reactions thermal analysis, X-ray photoelectron spectroscopy (XPS) and high-temperature XRD are performed. Based on these results a discussion will be given on densification and phase transformations during sintering of these nano–nano composites.

2. Experimental

2.1. Powder preparation and sintering study

Nanocrystalline 3 mol% yttria-doped stabilized tetragonal zirconia polycrystals (3Y-TZP) with a primary crystallite diameter of 8 nm were prepared by means of a co-precipitation method as described in.[14] CuO powders with a primary crystallite diameter of 15 nm were prepared by an oxalate complexation–precipitation method as described in.[12] The equivalent spherical diameter as calculated from the BET surface area, a measure for the aggregate size, were 10 and 50 nm for the 3Y-TZP and the CuO powder, respectively.[12] Composites of 3Y-TZP doped CuO were prepared by ball-milling appropriate amounts of powders in ethanol using zirconia balls as milling medium. The milled suspensions were ultrasonically dispersed for 5 min and oven-dried at 100 °C for 24 h. After grinding and sieving, the composite powders were pressed into cylindrical green compacts by isostatic pressing at 400 MPa for 5 min. The as-calcined 3Y-TZP powder (without CuO addition) also obtained the same milling, ultrasonic, drying and sieving treatment prior to compaction in order to obtain an identical powder morphology as the CuO-doped powders.

Compacts were sintered in a Netzsch dilatometer at 1130 °C for 1 h at a heating rate of 15 °C min^{-1} and a cooling rate of 2 °C min^{-1}. An extra 8 mol% CuO-doped 3Y-TZP sample was sintered at 960 °C for 20 h with a heating rate of 20 °C min^{-1}. Oxygen flow was introduced into the dilatometer while sintering.

A mixture of a fine-grained Y_2O_3–CuO powder with a Y/Cu atomic ratio of 1 was prepared by a citrate complexation/pyrolysis synthesis method. This powder mixture was used for high-temperature XRD analysis to detect any reaction between Y_2O_3 and CuO. For this citrate synthesis appropriate amounts of CuO (99.9% Aldrich Chemicals, Germany) and Y_2O_3 (99.9%, Merck Chemicals, Germany) were separately dissolved in nitric acid (HNO_3, 38%, Merck Chemicals, Germany). After mixing the two warm (80 °C) solutions, citric acid monohydrate ($C_6H_6O_7{\cdot}H_2O$, 99.9%, Merck chemicals, Germany) was added at a molecular ratio acid: (Cu + Y) = 1:1. After pH adjustment in a range between 6.5 and 7.0, by adding ammonia (NH_4OH, 65%, Merck Chemicals, Germany), the solution was heated to evaporate the solvent. It is important to avoid any precipitation and violent boiling during this evaporation procedure, otherwise stoichiometry is lost. When most of the solvent was removed the solution became dark-blue viscous and swelled upon further heating swelled and subsequently a strong combustion was ignited, leaving a foam-like brown powder. After slightly grinding in a plastic mortar the resulting powder was used for high-temperature X-ray diffraction analysis.

2.2. X-ray diffraction

High-temperature X-ray diffraction analysis (XRD, X'Pert_MPD, PANalytical, with Cu Kα1 radiation, λ = 1.542 Å, as X-ray source) data were collected in the 2θ range of 10–40° with a step size of 0.02°. During the measurement the sample was heated at 5 °C min^{-1} to the measuring temperature and held at that temperature for 15 min before the measurement started. X-ray diffraction was also used to analyse possible zirconia phase changes form tetragonal to monoclinic (or visa versa) after sintering of several % CuO-doped 3Y-TZP compacts. The volume fraction of monoclinic zirconia phase (V_m) was calculated based on the peak intensities using the relationship as proposed by Toraya et al.[15]

2.3. XPS analysis

The reactions during sintering of the CuO-doped 3Y-TZP nano-powder composites were further analysed by a series of X-ray photoelectron spectroscopy (XPS) analyses using a Quantera SXM from Physical Electronics, equipped with a monochromated Al Kα X-ray source, producing approximately 25 W of X-ray power on a spot with diameter of 100 μm. Spectra were referenced using the adventitious carbon C_{1s} peak at 284.8 eV. The analyzer was placed at an angle of 45° with the surface. Samples were neutralized during measurements using Ar ions and electrons. Element scans were measured using a pass energy of 112 eV and a step size of 0.2 eV.

For these experiments powder compacts of 8 mol% CuO-doped 3Y-TZP composites with 2–3 mm in thickness and 6–7 mm in diameter were prepared by isostatic pressing at 400 MPa for 5 min. XPS analysis were conducted on a fractured surface of a green (as-pressed) compact and on compacts sintered in oxygen at 600, 700 and 850 °C respectively for 30 min, with a heating rate of 15 °C min^{-1} and a cooling rate of 5 °C min^{-1}. XPS spectra were collected from both freshly fractured and slightly polished (with diamond paste as polishing media) surfaces of the sintered samples. Elemental composition of the surfaces was calculated on the basis of the spectra using Multipak software (version 8.0) from Physical Electronics.

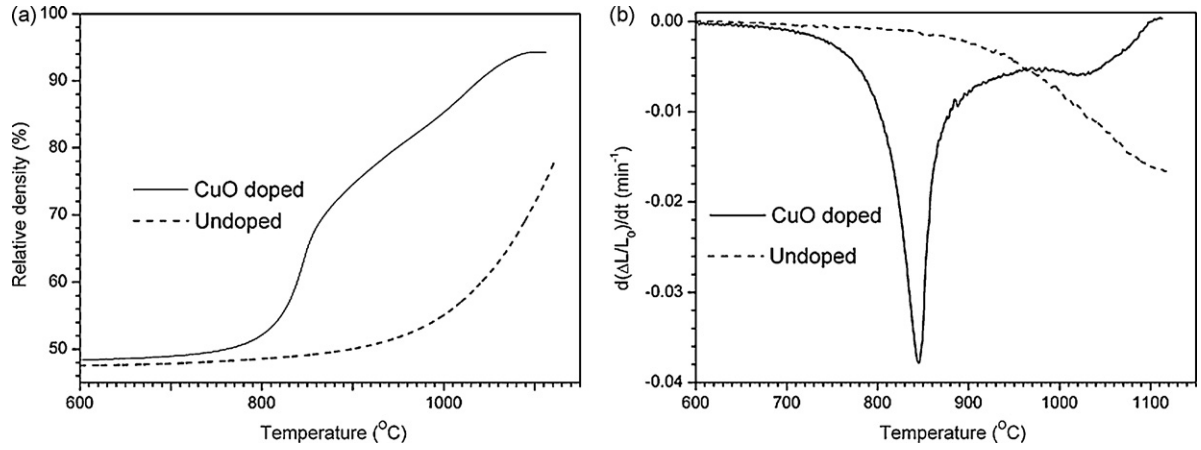

Fig. 1. Relative density (a) and linear shrinkage rate (b) of a pure nanocrystalline 3Y-TZP powder compact (dashed line) and an 8 mol% CuO-doped 3Y-TZP nano-composite (solid line).

2.4. Thermal analysis

Thermogravimetric analysis (TGA) and differential scanning calorimetric (DSC) measurement were carried out on compacts of undoped and 8 mol% CuO-doped 3Y-TZP powders using a Setaram Setsys 16 (Setaram, Cakuire, France). Powders were isostatically pressed into green compacts at 400 MPa for 5 min and subsequently slightly crushed into pieces, containing sufficient grain-grain interfaces to mimic sintering. For each TGA/DSC measurement approximately 25 mg compacted pieces were used. Single heating as well as cycled heating programs were used. During single heating experiments powder compacts were placed in a platinum cup and heated at 15 °C min^{-1} to 1100 °C (without measurements during dwell and cooling). It was observed that the compact reacts with the platinum cup at high temperatures (>1100 °C), which results in non-desired reactions and contamination of the equipment. Therefore further temperature-cycle measurements were conducted using an alumina cup as sample holder. Here the sample was first heated at 15 °C min^{-1} to 1150 °C and held at the maximum temperature for 30 min. After cooling at 5 °C min^{-1} to 600 °C the sample was reheated to 1150 °C at 15 °C min^{-1} followed by a dwell for 30 min. Finally the sample was cooled at 5 °C min^{-1} to room temperature. All thermal analysis experiments in this work were carried out in an (90% O_2 + 10% N_2) atmosphere for obtaining a similar environment as used for sintering studies on these CuO-doped 3Y-TZP nano-powder composites.

2.5. Microstructure

Scanning electron microscopy (SEM, Thermo Noran Instruments) was used for microstructure analysis on polished cross-sections of sintered samples. Prior to SEM experiments the samples sintered at 1130 °C were thermally etched at 1000 °C for 0.5 h. For the sample sintered at 960 °C thermal etching was carried out at 850 °C for 1 h. Average grain sizes were determined by the linear intercept technique based on the SEM images of the polished and thermally etched surfaces by using Mendelson's method.[16]

3. Results and discussion

In Fig. 1 the densification of compacts from single-phase nanocrystalline 3Y-TZP and an 8 mol% CuO-doped 3Y-TZP nanocomposite are compared. As can be seen from this figure the addition of this amount of nanocrystalline CuO drastically changes the sintering behaviour of nanocrystalline 3Y-TZP. The composite achieved a relative density of more than 95% just by heating to a temperature of 1100 °C (heating rate 15 °C/min), while single-phase nanocrystalline 3Y-TZP has a density of only 70% after the same temperature treatment. In a recent paper we described the sintering behaviour of a composite with the same composition but larger particle sizes (TZ3Y, Tosoh, BET equivalent diameter 60 nm and CuO, Aldrich, particle size ~5 μm).[4] These coarser-grained systems showed an opposite sintering behaviour meaning that the Y-TZP system is dense after heating to 1400 °C (heating rage 2 °C/min) while the 8 mol% CuO-doped compact achieved only a relative density >95% after sintering at 1500 °C for 8 h.

The most remarkable sintering results of the nano–nano composite are:

- Densification of the composite starts at 700 °C and shows a significant densification in the temperature range 820–860 °C, while pure nanocrystalline 3Y-TZP does not show any densification in this temperature range. A density increase from 56–70% is observed for the composite during a heating period of just 3 min.
- Above 860 °C densification of the composite is less fast, while the system is still in the intermediate stage of sintering. For normal single-phase sintering, like the 3Y-TZP system, there is a steady increase in density as function of temperature during heating until the final densification stage is achieved (at relative densities of 85–90%).

Another remarkable phenomenon for the CuO-doped nanocomposite is that the volume percentage of monoclinic zirconia started to increase while heating at ~860 °C or higher. Especially in the temperature range 900–1100 °C the amount

Table 1
Elemental composition of fractured and polished surfaces of 8 mol% CuO-doped 3Y-TZP as analysed by XPS.

ID	Sintering temperature (°C)	Measured surface	Atom % metallic elements		
			Cu(2p3)	Y(3d)	Zr(3d)
a	Unsintered	Fractured	9	7	84
b	600	Fractured	23	5	72
c	600	Polished	3	5	92
d	700	Fractured	26	5	69
e	700	Polished	2	5	93
f	850	Fractured	15	8	77
g	850	Polished	3	6	91

The bulk (overall) composition of 8 mol% CuO-doped 3Y-TZP is in atom %: 8% Cu, 5% Y and 87% Zr.

of monoclinic zirconia drastically increases to 80%, while the undoped pure 3Y-TZP remains fully tetragonal at these sintering temperatures.[13]

The observed "two-stage" sintering behaviour of the nano–nano composite was assumed to be caused by solid-state reactions which occur during heating of a powder compact.[13] However no experimental evidence was given for these reactions. Results of several analysis techniques are presented in this paper to elucidate these reactions. Now successively XPS, DSC/TGA and (high temperature) XRD results will be given. In Section 4 of this paper the sintering behaviour is analysed in terms of these reactions. Finally an explanation is given for the formation of monoclinic zirconia while heating a CuO-doped 3Y-TZP compact during sintering.

3.1. XPS analysis on CuO-doped 3Y-TZP nano-powder composite

Table 1 gives the atomic ratios of Cu, Y and Zr of a fractured surface of the as-pressed compact as well as fractured and polished surfaces of samples sintered at respectively 600, 700 and 850 °C. SEM analysis showed that all samples fracture along the grain boundaries. It is further assumed that polished cuts pass through the grains. Thus the elemental composition of the fractured and polished surfaces should well represent the composition of grain boundaries and grain bulk, respectively.

The composition of the as-pressed compact as analysed by XPS is in rather good agreement with the overall composition (see Table 1), implying a uniform dispersion of CuO in the 3Y-TZP matrix. The fractured surfaces of samples after sintering show a much higher Cu content than the nominal composition. On the other hand the polished surfaces of these samples contain less Cu if compared with the as-pressed sample.

More information on copper distribution on the fractured surfaces of the sintered samples is given by depth profile analysis. After a few minutes of Ar-ion sputtering (removing about 5 nm of the surface) all fractured surfaces of the sintered samples show a very rapid decrease in intensity of the Cu-signal (to less than 20%). These results reveal that copper enrichment is present in a several nm thin layer of the fractured surfaces.

A detailed XPS analysis of the Cu $3p_{3/2}$ signal was performed to shed more light on eventual reactions which result in copper enrichment at the grain boundaries during sintering. In Fig. 2 the result is given for a fractured sample sintered at 600 °C. Samples sintered at 700 or 800 °C show the same XPS pattern. An interesting observation is that for these sintered samples only one peak appears at a BE of 933 eV without the satellite at higher BE, whereas the Cu $2p_{3/2}$ spectra as measured on the unsintered specimen clearly showed a shakeup satellite peak at around 943 eV. The presence of a shakeup satellite peak combined with the Cu $2p_{3/2}$ main line at 934 eV is a typical feature of Cu with oxidation state (II). The special feature of Cu $2p_{3/2}$ spectrum as observed here, i.e. the absence of shakeup satellite, will be discussed later.

3.2. Thermal analysis of CuO-doped 3Y-TZP nano-powder composites

Fig. 3 shows TGA/DSC results of an 8 mol% CuO-doped 3Y-TZP sample measured with a single heating program. Besides the use of nanocrystalline powders instead of coarse-grained powders as used by Seidensticker and Mayo,[9] the way of sample preparation also differed with the work of these authors. In our work pressed powder compacts were used instead of loose powders resulting in a better interparticle contact so that reactions proceed in a way more comparable to sintering of a powder compact.

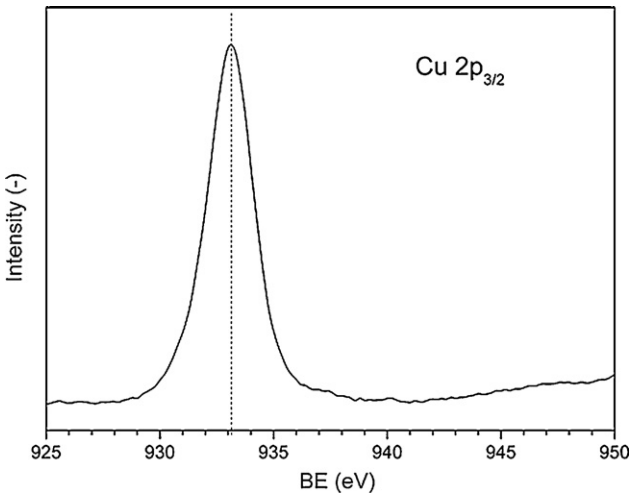

Fig. 2. Cu $2p_{3/2}$ spectrum of 8 mol% CuO-doped 3Y-TZP sintered at 600 °C.

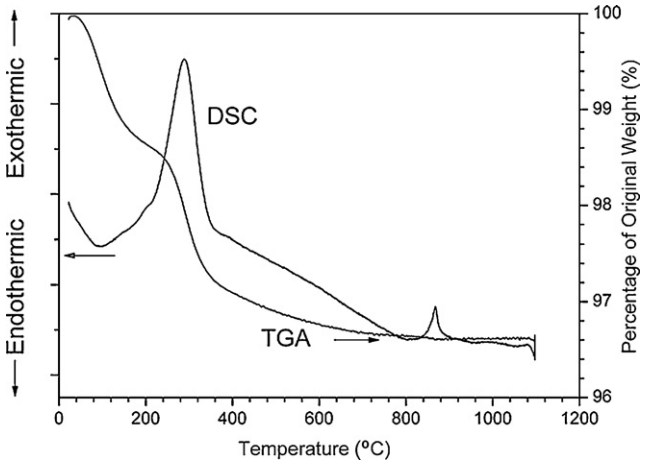

Fig. 3. Single heating TGA and DSC curves for 8 mol% CuO-doped 3Y-TZP, heated in 90% O_2 + 10% N_2; sample holder: platinum.

Between 100 and 400 °C an exothermic signal accompanied by a total weight loss of around 3% is observed for undoped and 3Y-TZP samples doped with CuO and can be attributed to desorption of water. At further heating a sharp exothermic peak, without any weight change, appears around 860 °C for the composite whereas no signal was found in this temperature range for undoped 3Y-TZP. This exothermic peak clearly points to a reaction between CuO and the 3Y-TZP. At around 1100 °C an endothermic reaction seems to start as indicated by the quick drop in the DSC signal at the end of this measurement.

Thermal analysis with a cycled temperature program was conducted for further characterization of reactions during sintering of the CuO-doped 3Y-TZP nano–nano composite and is given in Fig. 4. The signal at 860 °C is less intense as in Fig. 3, which is likely caused by the lower thermal conductivity of the alumina cup compared to the platinum cup used during the experiment as depicted in Fig. 3. An important feature of the reaction at 860 °C, as figured out by this cycled thermal analysis, is its irreversibility. As can be seen in Fig. 4 the DSC peak at 860 °C does not appear upon reheating.

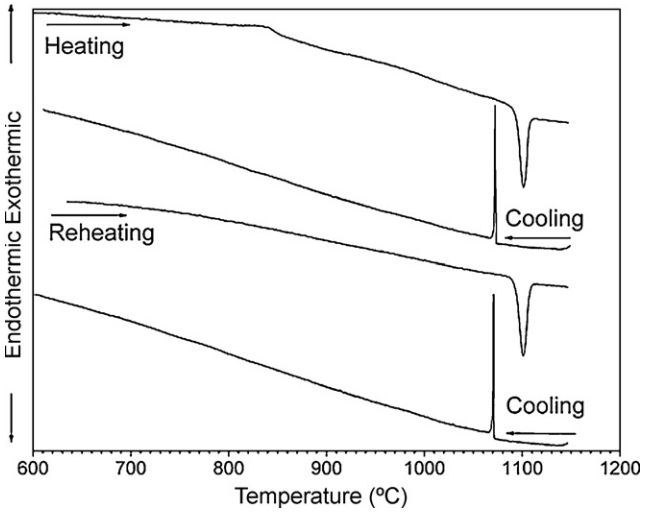

Fig. 4. Cycled DSC curve for 8 mol% CuO-doped 3Y-TZP, heated in 90% O_2 + 10% N_2; sample holder: alumina cup.

The endothermic reaction at around 1100 °C can completely be observed in the cycled thermal analysis, while during cooling an exothermic signal was observed in the same temperature region. During the second cycle of heating and cooling the reactions at around 1100 °C occurred in the same way. These endothermic and exothermic signals can be ascribed to respectively melting and solidification of $Y_2Cu_2O_5$ as was also observed in the same temperature region by Mayo et al.[10] and Gadalla and Kongkachuichay.[17] The formation of $Y_2Cu_2O_5$ in our system will be discussed in Section 4 of this paper.

3.3. Analysis of reactions between Y_2O_3 and CuO during heating

According to the pseudo-binary phase diagram of the Y_2O_3–CuO system in air, a reaction between Y_2O_3 and CuO takes place around 900 °C, resulting in the formation of an yttria-copper-oxide phase.[17] In ZrO_2–Y_2O_3 solid solutions Y tends to segregate to the grain boundaries at elevated temperatures (≥800 °C).[18] It was proposed in literature that a reaction takes place between CuO and yttria as segregated to the 3Y-TZP grain boundaries, to form an yttria-copper-oxide phase during sintering[9–11] of CuO-doped 3Y-TZP systems. This reaction could be of importance for the sintering behaviour and microstructure evolution of the material. Detailed characteristics of this reaction were not reported yet and will be given here.

High-temperature XRD measurements were performed on a representative system, i.e. a powder mixture of Y_2O_3 and CuO. The reactions in the powder mixture of fine-grained CuO and Y_2O_3 as prepared by the citrate synthesis route is well representing the reactions between CuO and yttria as segregated to the 3Y-TZP grain boundary in our nano composite.

Fig. 5 shows the XRD patterns of the Y_2O_3–CuO powder mixture at various temperatures. The starting powder can be very well characterized as a mixture of CuO and Y_2O_3. All signals from this pattern can be indexed to reflections of CuO and Y_2O_3, except a minor peak at around 2θ of 31°. This signal can be ascribed to a small amount of $Y_2Cu_2O_5$ which was formed by pyrolysis during the citrate synthesis. As indicated by the broad width of the peaks, both CuO and Y_2O_3 particles in this mixed powder are very fine. While heating the XRD pattern does not change until 750 °C except a slight shift of the peaks towards lower 2θ due to thermal expansion of the lattices. However, at 800 °C the peaks of both CuO and Y_2O_3 start to decrease in intensity and signals of $Y_2Cu_2O_5$ appear (at 2θ of around 29.8, 30.6 and 32.6°, respectively), although at very small intensities. This clearly indicates that a solid-state reaction starts around 800 °C resulting in the formation of $Y_2Cu_2O_5$. At further heating more $Y_2Cu_2O_5$ is formed, while at 950 °C only $Y_2Cu_2O_5$ can be observed, indicating completion of the reaction. After cooling to room temperature (=end) the sample shows an identical XRD pattern as that at 950 °C, revealing the irreversibility of the formation of $Y_2Cu_2O_5$.

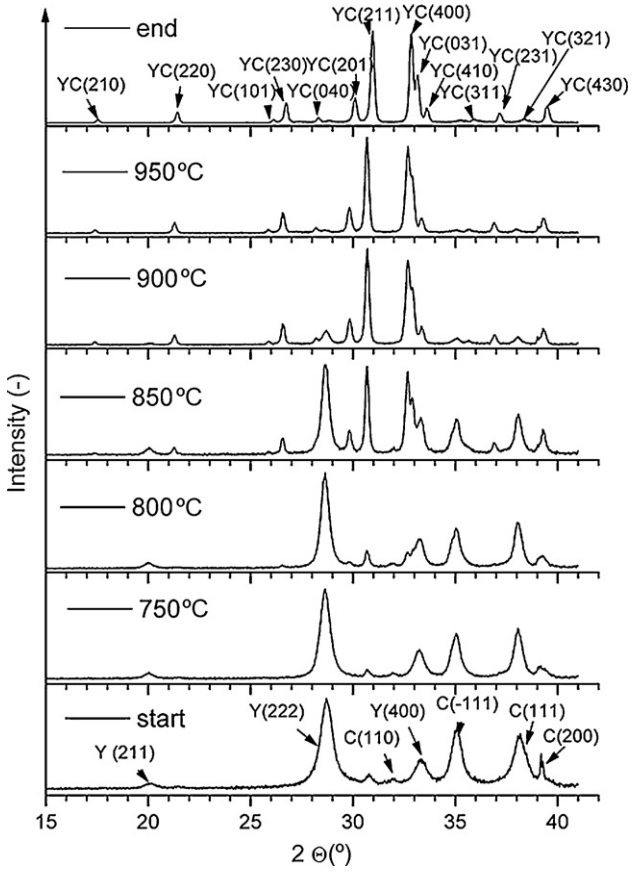

Fig. 5. XRD patterns of Y_2O_3 + CuO powder mixture at various temperatures. Y, C and YC denote reflections of Y_2O_3, CuO and $Y_2Cu_2O_5$ phases respectively; Patterns marked as "start" and "end" are measured at room temperature before heating and after cooling, respectively.

4. General discussion on sintering of CuO-doped 3Y-TZP nano–nano composites

As described in the previous section several reactions occur during sintering of the CuO-doped 3Y-TZP nano-composite powder compacts. The influence of those reactions on sintering will now be discussed.

XPS results indicate a strong enrichment of Cu in the 3Y-TZP grain-boundary layer after sintering at 600 °C (Table 1). Furthermore a change in the Cu $2p_{3/2}$ XPS spectrum (disappearing of shakeup satellite peak) was observed. These observations give insight in the reactions resulting in Cu-enrichment in the grain boundaries.

One possible explanation of the absence of a shakeup signal of Cu $2p_{3/2}$ (see Fig. 2) is the reduction of Cu^{2+} to Cu^{1+}, i.e. dissociation of CuO to Cu_2O.[19] However, this reduction only occurs around 1050 °C.[3,17] Additionally the BE of the Cu $2p_{3/2}$ main line (around 933 eV) indicates that the oxidation state of copper species should nevertheless be essentially Cu(II), because it is remarkably higher than that of Cu (I) (931 eV).[19] The Cu $2p_{3/2}$ XPS spectrum of the sintered specimen is more likely to be associated a dissolution of CuO in the grain boundary of 3Y-TZP. Dongare et al.[20] reported that this shakeup feature disappears if Cu^{2+} is substituted on Zr^{4+} sites in the zirconia lattice and that the BE of Cu $2p_{3/2}$ shifts to only a slightly lower value (933.4 eV) due to the association between Cu $2p_{3/2}$ and electron holes created by oxygen vacancies in the zirconia lattice. The good similarity between our results and Dongare's observation proves that dissolution of CuO in the 3Y-TZP lattice occurs in our system when it is sintered at 600 °C.

It is obvious that CuO dissolution starts at contact points between CuO and 3Y-TZP grains, while the dissolved copper species further diffuse along the 3Y-TZP grain boundaries driven by chemical concentration gradients. In the case of the composite as studied in the present work both 3Y-TZP and CuO grains are on nanometer scale, which means large amounts of contact area between CuO and 3Y-TZP grains are present in the material and therefore a fast dissolution of Cu in the Y-TZP grain occurs.

The exothermic DSC signal at 860 °C (Figs. 3 and 4) is clearly caused by an irreversible reaction between CuO and the 3Y-TZP grains. A similar irreversible exothermic signal was also observed by Seidensticker and Mayo[9] and Hayakawa et al.[11] on their study of CuO-doped 3Y-TZP systems. Seidensticker did not assign any reaction to this signal. Hayakawa attributed this signal to the reaction between CuO and yttria resulting in the formation of $Y_2Cu_2O_5$ but these authors did not provide any additional evidence for this reaction. Comparing DSC and high-temperature XRD results as shown in Figs. 4 and 5 respectively, it is justified that during sintering around 860 °C $Y_2Cu_2O_5$ is formed in the composite, which is in a good agreement with Hayakawa's[11] conclusions.

The reactions discussed in this paper have significant influences on sintering and microstructure evolution of the CuO-doped 3Y-TZP system. We will now discuss the sintering results as depicted in Fig. 1 in relation with those reactions. First the fast densification behaviour between 700 and 860 °C will be treated.

The dissolution of CuO in 3Y-TZP can result in an increase in both lattice defects in the grain-boundary area as well as the formation of a cubic zirconia phase.[10,20] Both these phenomena and the dissolution process of Cu in the zirconia phase itself significantly increases ion diffusivity in the 3Y-TZP grains, especially in the grain boundary. As grain boundary diffusion normally plays an important role in densification during sintering, an increased ion diffusivity strongly enhances the initial and intermediate stages of sintering, and consequently result in a low onset temperature for sintering. The striking fast densification between 820 and 860 °C can be explained by a "transient" liquid-phase sintering mechanism. The dissolution of Cu in the 3Y-TZP grain boundaries as described above easily results in the formation of a very thin (a few atomic layers thick) amorphous ("transient" liquid) layer at the grain boundaries.

For the CuO/3Y-TZP composite a decrease in densification rate is observed at 860 °C, while sintering is far from complete at that temperature (Fig. 1). This sudden decrease in the intermediate stage of sintering is most probably caused by the reaction where $Y_2Cu_2O_5$ is formed. It is assumed that this solid phase removes the liquid grain-boundary phase and subsequently a decrease in sintering rate occurred above 860 °C.

Table 2
Volume percentage of monoclinic zirconia of undoped and CuO-doped 3Y-TZP nano–nano composites after a sintering procedure as indicated.

CuO (mol%)	Sintering procedure[a]	Density (% rel)[b]	V_m (%)
0	15 – 1150 × 2 h – 2	93	0
0.8	15 – 1130 × 1 h – 2	98	79
1.6	15 – 1130 × 1 h – 2	95	79
3.2	15 – 1130 × 1 h – 2	94	78
8	15 – 1130 × 1 h – 2	93	79
8	20 – 960 × 20 h – 2	96	79

[a] Heating rate (°C/min) – maximum temperature (°C) × holding time (h) – cooling rate (°C/min).
[b] For density calculation (ρ_{rel} in % of the theoretical density) the ratio tetragonal to monoclinic zirconia was taken into account in calculating the theoretical density.

Another reason might be that the formed $Y_2Cu_2O_5$ is present as a thin layer, partly or completely covering the 3Y-TZP grains, which acts as a barrier to matter diffusion between Y-TZP grains.

A phenomenon, which is very remarkable during sintering of this nanocomposite, is the phase transformation from tetragonal to monoclinic zirconia when heating above 900 °C.[13] During cooling the CuO-doped sample showed no further phase transformation, indicating that the zirconia phase transformation has been completed during the heating process. This latter is confirmed in two ways. An XRD pattern of a sintered sample taken at room temperature showed 79% of monoclinic zirconia. Secondly, as shown in Fig. 6, the dilatometer experiment showed no (sudden) expansion due to a martensitic tetragonal to monoclinic phase transformation. Additional experiments showed that the addition of only a small amount of CuO (0.8 mol%) to the nanocrystalline 3Y-TZP powders already results in the presence of about 80 vol.% monoclinic zirconia in the ceramic. Table 2 shows that, independently of the amount of CuO added, 3Y-TZP CuO nano–nano composites reveal approximately 80 vol.% monoclinic zirconia after sintering, while the pure (undoped) 3Y-TZP ceramic remains 100% tetragonal after the same sintering procedure.

As a/o described by Yashima et al.[21] the monoclinic (m) phase is the thermodynamic stable phase at temperatures <1200 °C for 3Y-TZP. However the non-equilibrium tetragonal (t) phase can be stabilized <1200 °C by an energy barrier ΔG^* (i.e. stabilization by kinetics).[22] As stated in[21,23] the phase stability is strongly affected by chemical reactions, which e.g. changes the oxygen stoechiometry. These chemical reactions increase kinetics and consequently drastically decrease the kinetic energy barrier for phase transformation ΔG^*. Under those circumstances phase composition is (mainly) determined by thermodynamic stabilization through the free energy–energy difference ΔG.[21] The reaction between the CuO phase and Y_2O_3 from the 3Y-YZP phase by forming $Y_2Cu_2O_5$, which starts around 860 °C, can therefore explain that the thermodynamic stable mono-

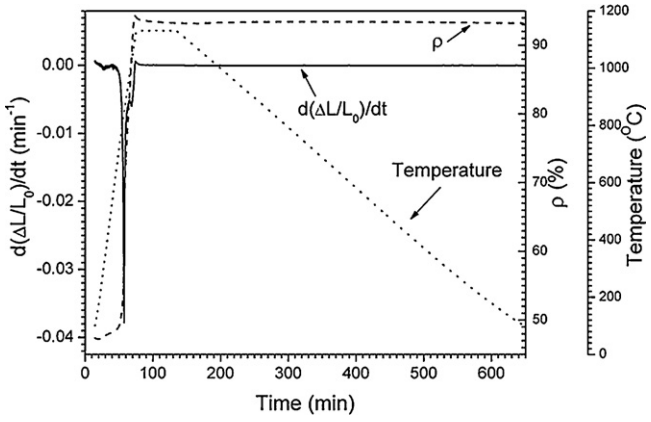

Fig. 6. Relative density and linear shrinkage of the CuO-doped nanocomposite during a dilatometer experiment; *note*: no change in dimensions occur during cooling.

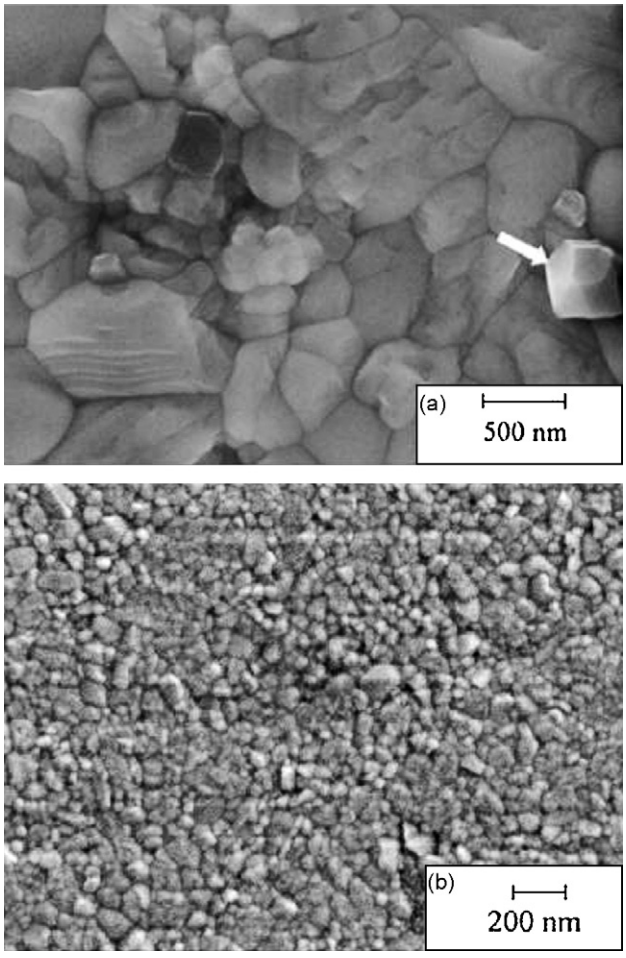

Fig. 7. SEM picture of a polished and thermally etched 8 mol% CuO-doped 3Y-TZP nano-powder compact; (a) after sintering for 2 h at 1130 °C (heating rate 15 °C/min); (b) after sintering for 20 h at 960 °C (heating rate 20 °C/min).

clinic phase is obtained during heating from 860 to 1100 °C, while for the pure single-phase 3Y-TZP ceramic the meta stable tetragonal phase remains.[13] In all cases described in this paper the maximum sintering temperature is <1200 °C, meaning that for the composite the (thermodynamically favourable) m → t phase transitions does not occur during heating, while during cooling also no phase transitions occur (Fig. 6 and Table 2).

Finally grain growth will be shortly discussed. After the dilatometer experiment SEM pictures of polished and thermally etched composite has a structure as given in Fig. 7a. The sample showed a non-uniform microstructure with irregularly shaped grains up to several micrometers and grains with a size of around 200 nm. Also some pure CuO grains were observed by EDX (e.g. the grain indicated by an arrow in Fig. 7a). However, a pure 3Y-TZP sample, made from the nanocrystalline powder, exhibits a uniform microstructure with grains of 150 nm after the same sintering procedure.[24] As shown in this paper a nanocomposite powder compact of 3Y-TZP doped with 8 mol% CuO shows a very fast densification at a relative low temperature (<900 °C; see e.g. Fig. 1). Using this knowledge we performed a (preliminary) sintering experiment where a powder compact was sintered at 960 °C for 20 h (heating rate 20 °C min^{-1}). The material has a real nanostructured microstructure consisting of uniformly small grains of 120 nm. This final result clearly shows that a dense CuO-doped 3Y-TZP ceramic without significant grain growth is successfully obtained by well controlling the sintering procedure.

5. Conclusions

The abundance of reactions, which occur during sintering of CuO-doped 3Y-TZP nano-powder composites were comprehensively investigated. A strong dissolution of CuO in the 3Y-TZP matrix below 600 °C was proven by XPS analysis, resulting in an enrichment of Cu in the 3Y-TZP grain boundaries. This dissolution results in a unique fast densification between 700 and 860 °C caused by a "metastable transient liquid phase" mechanism. A reaction between CuO and yttria as segregated to the 3Y-TZP grain boundaries at around 860 °C forming $Y_2Cu_2O_5$ was clarified by a combination of thermal analysis and high-temperature XRD analysis. This reaction enhances the formation of monoclinic zirconia, by reducing the kinetic energy barrier for phase transformation (ΔG^*), while the solid product formed retards densification.

It can be concluded that the CuO dissolution in 3Y-TZP is beneficial for sintering of the CuO-doped 3Y-TZP nano-powder composites, whereas the formation of $Y_2Cu_2O_5$ is detrimental. Based on these results a (preliminary) sintering experiment was performed at 960 °C for 20 h (heating rate 20 °C min^{-1}) resulting in a dense CuO-doped 3Y-TZP ceramic with grain size of 120 nm.

Acknowledgements

The Dutch Technology Foundation (STW) is gratefully acknowledged for the financial support. Mrs. Mieke Luitenolieman and Mrs. Cindy Huiskes are acknowledged for the DSC/TGA experiments.

References

1. Hwang, C. M. J. and Chen, I.-W., Effect of a liquid phase on superplasticity of 2-mol%-Y_2O_3-stabilized tetragonal zirconia polycrystals. *J. Am. Ceram. Soc.*, 1990, **73**(6), 1626–1632.
2. Kerkwijk, B., García, M., van Zyl, W. E., Winnubst, L., Mulder, E. J., Schipper, D. J. *et al.*, Friction behaviour of solid oxide lubricants as second phase in α-Al_2O_3 and stabilised ZrO_2 composite. *Wear*, 2004, **256**(1–2), 182–189.
3. Pasaribu, H. R., Sloetjes, J. W. and Schipper, D. J., Friction reduction by adding copper oxide into alumina and zirconia ceramics. *Wear*, 2003, **255**(1–6), 699–707.
4. Ran, S., Winnubst, A. J. A., Blank, D. H. A., Pasaribu, H. R., Sloetjes, J.-W. and Schipper, D. J., Effect of microstructure on the tribological and mechanical properties of CuO-doped 3Y-TZP ceramics. *J. Am. Ceram. Soc.*, 2007, **90**(9), 2747–2752.
5. Ran, S., Winnubst, A. J. A., Wiratha, W. and Blank, D. H. A., Sintering behavior of 0.8 mol%-CuO-doped 3Y-TZP ceramics. *J. Am. Ceram. Soc.*, 2006, **89**(1), 151–155.
6. Ramesh, S., Gill, C. and Lawson, S., The effect of copper oxide on sintering, microstructure, mechanical properties and hydrothermal ageing of coated 2.5Y-TZP ceramics. *J. Mater. Sci.*, 1999, **34**, 5457–5467.
7. Lemaire, L., Scholz, S. M., Bowen, P., Dutta, J., Hofmeister, H. and Hofmann, H., Effect of CuO additives on the reversibility of zirconia crystalline phase transitions. *J. Mater. Sci.*, 1999, **34**, 2207–2215.
8. Kimura, N., Okamura, H. and Morishita, J., Preparation of Y_2O_3-TZP by low-temperature sintering. *Adv. Ceram.*, 1988, **24**, 183–191.
9. Seidensticker, J. R. and Mayo, M. J., Thermal analysis of 3-mol%-yttria-stabilized tetragonal zirconia powder doped with copper oxide. *J. Am. Ceram. Soc.*, 1996, **79**(2), 401–406.
10. Mayo, M. J., Seidensticker, J. R., Hauge, D. C. and Carim, A. H., Surface chemistry effects on the processing and superplastic properties of nanocrystalline oxide ceramics. *Nanostruct. Mater.*, 1999, **11**(2), 271–282.
11. Hayakawa, M., Inoue, T., Pee, J.-H., Suematsu, H. and Yamauchi, H., Liquid phase sintering of Y-TZP with CuO and $Y_2Cu_2O_5$ dopants. *Mater. Sci. Forum*, 1999, **304–306**, 465–470.
12. Ran, S., Winnubst, A. J. A., Wiratha, W. and Blank, D. H. A., Synthesis, sintering and microstructure of 3Y-TZP/CuO nano-powder composites. *J. Eur. Ceram. Soc.*, 2006, **26**(1), 391–396.
13. Ran, S., Winnubst, A. J. A., Koster, H., de Veen, P. J. and Blank, D. H. A., Sintering behaviour and microstructure of 3Y-TZP + 8 mol% CuO nano-powder composite. *J. Eur. Ceram. Soc.*, 2007, **27**(2–3), 683–687.
14. Groot Zevert, W. F. M., Winnubst, A. J. A., Theunissen, G. S. A. M. and Burggraaf, A. J., Powder preparation and compaction behaviour of fine-grained Y-TZP. *J. Mater. Sci.*, 1990, **25**(11), 3449–3455.
15. Toraya, H., Yoshimura, M. and Somiya, S., Calibration curve for quantitative analysis of the monoclinic-tetragonal ZrO_2 system by X-ray diffraction. *J. Am. Ceram. Soc.*, 1984, **67**(6), C119–C121.
16. Mendelson, M. I., Average grain size in polycrystalline ceramics. *J. Am. Ceram. Soc.*, 1969, **52**, 443–446.
17. Gadalla, A. M. and Kongkachuichay, P., Compatible phases of the Y_2O_3–CuO–Cu_2O system in air. *J. Mater. Res.*, 1991, **6**, 450–454.
18. Burggraaf, A. J., van Hemert, M., Scholten, D. and Winnubst, A. J. A., Chemical composition of oxidic interfaces in relation with electric and electrochemical properties. In *Reaction of Solids*, ed. P. Barret and L. C. Dufour, 1985, pp. 797–802.
19. Handbook of X-ray photoelectron spectroscopy: a reference book of standard spectra for identification and interpretation of XPS data. In ed. J. Chastain. Eden Prairie, Minnesota, USA, 1992.
20. Dongare, M. K., Dongare, A. M., Tare, V. B. and Kemnitz, E., Synthesis and characterization of copper-stabilized zirconia as an anode material for SOFC. *Solid State Ionics*, 2002, **152/153**, 455–462.

21. Yashima, M., Kakihana, M. and Yoshimura, M., Metastable-stable phase diagrams in the zirconia-containing systems utilized in solid-oxide fuel cell application. *Solid State Ionics*, 1996, **86–88**, 1131–1149.
22. Yoshimura, M., Phase stability of zirconia. *Am. Ceram. Soc. Bull.*, 1988, **67**(12), 1950–1955.
23. Yashima, M., Morimoto, K., Ishizawa, N. and Yoshimura, M., Diffusionless tetragonal-cubic transformation temperature in zirconia-ceria solid solutions. *J. Am. Ceram. Soc.*, 1993, **67**(11), 2865–2868.
24. Theunissen, G. S. A. M., Winnubst, A. J. A. and Burggraaf, A. J., Sintering kinetics and microstructure development of nanoscale Y-TZP ceramics. *J. Eur. Ceram. Soc.*, 1993, **11**(7), 315–324.